

2. H. Haberland, *Surf. Sci.* **156**, 305 (1985).
3. J. Gspann and H. Vollmer, in *Rarefied Gas Dynamics*, K. Karamcheti, Ed. (Academic Press, New York, 1974), pp. 261–267.
4. J. Cuvelier *et al.*, *Z. Phys. D* **21**, 265 (1991).
5. M. Lewerenz, B. Schilling, J. P. Toennies, *Chem. Phys. Lett.* **206**, 381 (1993).
6. A. De Martino *et al.*, *Z. Phys. D* **27**, 185 (1993).
7. U. Buck and H. Meyer, *J. Chem. Phys.* **84**, 4854 (1986).
8. B. L. Bewig, U. Buck, Ch. Mehlmann, M. Winter, *ibid.* **100**, 2765 (1994).
9. O. Carnal, A. Faulstich, J. H. Mlynek, *Appl. Phys. B* **53**, 88 (1991).
10. D. W. Keith, M. L. Schattenburg, H. I. Smith, D. E. Pritchard, *Phys. Rev. Lett.* **61**, 1580 (1988).
11. D. W. Keith, R. J. Soare, M. J. Rooks, *J. Vac. Sci. Technol.* **89**, 2846 (1991).
12. F. Luo, G. C. McBane, G. Kim, C. F. Giese, W. R. Gentry, *J. Chem. Phys.* **98**, 3564 (1993); R. A. Aziz and M. J. Slaman, *ibid.* **94**, 8647 (1991).
13. J. B. Anderson, C. A. Traynor, B. M. Boghosian, *ibid.* **99**, 345 (1993).
14. D. Pritchard, personal communication; J. Schmiedmayer *et al.*, in preparation; M. S. Chapman *et al.*, *Interferometry with Atoms and Molecules*, vol. 9 of *OSA Technical Digest Series* (Optical Society of America, Washington, DC, 1994), p. 35.
15. From the observed disappearance of the dimer peak at high pressures ( $T_0 = 30$  K), we can rule out the possibility of a spurious peak that is a result of grating damage as reported in (10).
16. E. S. Meyer, J. C. Mester, I. F. Silvera, *J. Chem. Phys.* **100**, 4021 (1994).
17. F. Luo, G. C. McBane, G. Kim, C. F. Giese, W. R. Gentry, *ibid.*, p. 4023.
18. E. Buonomo, F. A. Gianturco, F. Ragnetti, W. Schöllkopf, J. P. Toennies, unpublished results.
19. V. Efimov, *Phys. Lett.* **338**, 563 (1970).
20. Th. Cornelius and W. Glöckle, *J. Chem. Phys.* **85**, 3906 (1986).
21. J. W. Gibbs, *Trans. Connecticut Acad.* **3**, 108 (1876); M. Vollmer and A. Weber, *Z. Phys. Chem.* **119**, 277 (1926); R. Becker and W. Döring, *Ann. Phys.* **24**, 719 (1935).
22. S. Kotake and I. I. Glass, *Prog. Aerosp. Sci.* **19**, 129 (1981).
23. D. R. Miller, in *Atomic and Molecular Beam Methods*, G. Scoles, Ed. (Oxford, New York, 1988).
24. S. Weisgerber and P.-G. Reinhard, *Z. Phys. D* **23**, 275 (1992); M. Barranco, D. M. Jezek, E. S. Hernández, J. Navarro, Ll. Serra, *ibid.* **28**, 257 (1993).
25. U. Buck, *J. Phys. Chem.* **92**, 1023 (1988).
26. J. M. Carter, D. B. Olster, M. L. Schattenburg, A. Yen, H. I. Smith, *J. Vac. Sci. Technol. B* **10**(6), 2909 (1992).
27. A. Yen, M. L. Schattenburg, H. I. Smith, *Appl. Opt.* **31**, 2972 (1992).
28. We thank D. Pritchard and his colleagues and C. Ekstrom and M. Chapman for lending us the 200-nm grating for these experiments and for advice on handling. We are also grateful to J. Harms and U. Henne for stimulating discussions and assistance with the experiments.

## RESEARCH ARTICLE

# Calcium-Calmodulin Modulation of the Olfactory Cyclic Nucleotide-Gated Cation Channel

Mingyao Liu,\*† Tsung-Yu Chen,\*‡ Basheer Ahamed, Jess Li, King-Wai Yau§

Although several ion channels have been reported to be directly modulated by calcium-calmodulin, they have not been conclusively shown to bind calmodulin, nor are the modulatory mechanisms understood. Study of the olfactory cyclic nucleotide-activated cation channel, which is modulated by calcium-calmodulin, indicates that calcium-calmodulin directly binds to a specific domain on the amino terminus of the channel. This binding reduces the effective affinity of the channel for cyclic nucleotides, apparently by acting on channel gating, which is tightly coupled to ligand binding. The data reveal a control mechanism that resembles those underlying the regulation of enzymes by calmodulin. The results also point to the amino-terminal part of the olfactory channel as an element for gating, which may have general significance in the operation of ion channels with similar overall structures.

Ion channels are subject to modulation that enhances their functional flexibility by various noncovalent or covalent structural modifications, the most common being phosphorylation by protein kinases (1). These modifications can alter voltage- or ligand-sensitivity, probability of opening,

rate of desensitization or inactivation, or other properties (1). Among ion channel modulations, one unusual form involves an apparently direct interaction between calcium-calmodulin ( $\text{Ca}^{2+}$ -CaM) and the channel protein. Channels showing this property include  $\text{Ca}^{2+}$ -dependent sodium and potassium channels in *Paramecium* (2), the ryanodine receptor channel in muscle (3), and a  $\text{K}^+$  channel in kidney (4). More recently, the cyclic nucleotide-activated cation channels mediating visual and olfactory transductions have also been found to be apparently modulated directly by  $\text{Ca}^{2+}$ -CaM (5, 6). The modulation of the olfactory channel is particularly pronounced, with the apparent affinity of the channel for cyclic nucleotide reduced by more than an

order of magnitude in the presence of  $\text{Ca}^{2+}$ -CaM (6), a property probably important for olfactory adaptation (7, 8). The retinal and olfactory channels share features with voltage-activated, Shaker-type  $\text{K}^+$  channels, including six putative transmembrane domains (one being an S4-like domain), cytoplasmic amino and carboxyl termini, and a conserved pore-forming region (9–11). One distinctive feature of the retinal and olfactory channels, however, is a cyclic nucleotide-binding site in the COOH-terminal segment which, when bound to ligand, leads to activation of the channel (9, 10). Both the native rod and olfactory channels are composed of  $\alpha$  and  $\beta$  subunits (also called subunits 1 and 2) that have 30 to 50 percent amino acid identity and a similar hydropathy pattern, even though only the  $\alpha$  subunit can form functional cyclic nucleotide-activated ion channels by itself (12, 13). The wealth of structural and functional information about these channels offers an opportunity to examine their modulation by  $\text{Ca}^{2+}$ -CaM more closely. We report here experiments on the olfactory channel to define the site where  $\text{Ca}^{2+}$ -CaM binds as well as the molecular nature of the modulation. We have identified a domain on the channel protein that contributes to high apparent ligand affinity. When  $\text{Ca}^{2+}$ -CaM binds to the same general domain, the influence of the domain is removed, leading to a decrease in apparent affinity for ligand. We also discovered that the  $\text{NH}_2$ -terminus of the olfactory channel affects gating.

**Identification of the CaM binding site.** Our previous work indicated that the homo-oligomeric channel formed by the  $\alpha$  subunit of the rat olfactory cyclic nucleotide-activated channel (which we call the olfactory channel) is strongly modulated by  $\text{Ca}^{2+}$ -CaM (6). At the same time, the  $\alpha$  subunit of the rod guanosine 3',5'-monophosphate (cyclic GMP)-activated channel (which we call the rod channel) neither

M. Liu, B. Ahamed, J. Li, and K.-W. Yau are in the Howard Hughes Medical Institute, T.-Y. Chen and K.-W. Yau are in the Department of Neuroscience, and K.-W. Yau is also in the Department of Ophthalmology, Johns Hopkins University School of Medicine, Baltimore, MD 21205, USA.

\*These authors made equal contributions to this work.

†Present address: Division of Biology, California Institute of Technology, Pasadena, CA 91125, USA.

‡Present address: Department of Biochemistry, Brandeis University, Waltham, MA 02254, USA.

§To whom correspondence should be addressed.

binds nor is sensitive to  $\text{Ca}^{2+}$ -CaM (5). First we showed that  $\text{Ca}^{2+}$ -CaM bound to the olfactory channel. The complementary DNA (cDNA) encoding this channel in rat was transfected into HEK293 cells, and total membrane proteins from the transfected cells were separated by SDS-polyacrylamide gel electrophoresis (SDS-PAGE) and assayed for CaM binding with  $^{125}\text{I}$ -labeled CaM in the presence of  $\text{Ca}^{2+}$  (14). Several proteins bound  $\text{Ca}^{2+}$ -CaM (Fig. 1A). However, compared to control transfections with the pCIS expression vector alone or with the rod channel cDNA, transfection with the olfactory channel cDNA gave an extra labeled band at approximately 76 kD, close to the calculated molecular mass of the protein. The labeling of this band was absent if EGTA was present in place of  $\text{Ca}^{2+}$ .

To localize the CaM-binding region on the olfactory channel, we used chimeras in which the  $\text{NH}_2$ -terminal part came from the corresponding region of the rat olfactory channel and the remainder from that of the human rod channel (Fig. 1B, top) (15). The cDNAs encoding these chimeras were transfected separately into HEK293 cells, and the expressed homo-oligomeric channels were tested for CaM sensitivity with patch-clamp recording on excised, inside-out membrane patches (16). In all cases, the membrane current induced by a non-saturating concentration of cyclic GMP was reduced by  $\text{Ca}^{2+}$ -CaM (Fig. 1B, bottom). These experiments, particularly the one with chimera 3, indicate that the cytoplasmic  $\text{NH}_2$ -terminal segment of the olfactory channel is important for CaM modulation and also contains the CaM binding site.

To confirm CaM binding to the  $\text{NH}_2$ -terminal, a fusion protein composed of the cytoplasmic  $\text{NH}_2$ -terminal segment of the rat olfactory channel and glutathione-S-transferase (GST) was constructed in pGEX-2T plasmid and expressed in bacteria, and the expression product was affinity-purified with glutathione-agarose beads or on a column (17). After SDS-PAGE, an overlay with  $^{125}\text{I}$ -labeled CaM was again performed. This fusion protein bound  $\text{Ca}^{2+}$ -CaM (Fig. 1C, left lane); no CaM binding was observed in the absence of  $\text{Ca}^{2+}$ . Experiments with fusion proteins containing the COOH-terminal segment of the olfactory channel, the  $\text{NH}_2$ - and COOH-terminal segments of the human rod channel, or the GST backbone gave no evidence of labeling.

Examination of the  $\text{NH}_2$ -terminal segment of the rat olfactory channel reveals a putative CaM-binding domain, Arg<sup>62</sup>-Arg<sup>87</sup>, that is characterized by two aromatic or long-chain aliphatic residues separated by 12 amino acids, many of which are positively charged (Fig. 2A). These features are present in known CaM-binding sites of sev-

eral proteins such as myosin light chain kinase and in CaM-binding peptides including mellitin and mastoparan (18). In an  $\alpha$ -helical wheel (Fig. 2B), the identified domain shows a basic amphiphilic structure that is also thought to favor CaM binding (19). An amphiphilicity profile of the  $\text{NH}_2$ -terminal segment points to the same region (Fig. 2C). Domains with some of these features can also be detected elsewhere in the protein sequence and are not necessarily indicative of true CaM-binding sites. Accordingly, we deleted the 26-amino acid domain in Fig. 2A from the  $\text{NH}_2$ -terminal

fusion protein described above; a CaM-binding assay indicated that this deletion mutant did not bind  $\text{Ca}^{2+}$ -CaM (Fig. 2D). Deletions of other regions of the fusion protein retained CaM-binding. When the cDNA encoding the entire channel protein missing a region containing Arg<sup>62</sup>-Arg<sup>87</sup> was transfected into HEK293 cells, subsequent assay of the membrane proteins indicated that the labeled band of appropriate molecular size detected for the wild-type channel was also absent (Fig. 2E). Thus, the Arg<sup>62</sup>-Arg<sup>87</sup> domain appears to be the only CaM-binding site on the olfactory channel. This domain

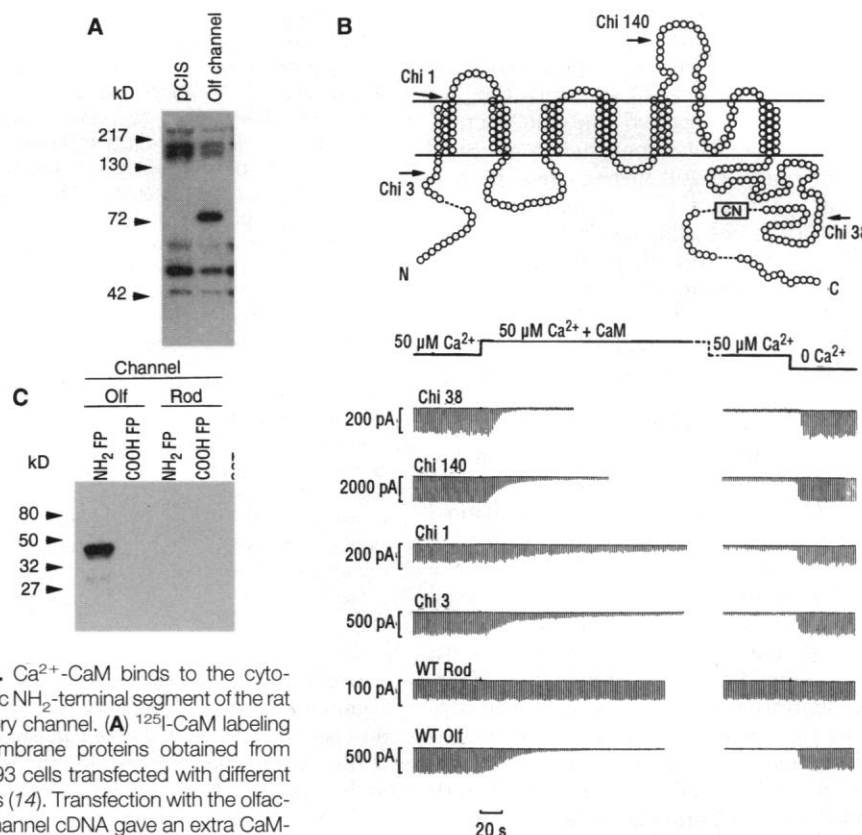


**Fig. 1.**  $\text{Ca}^{2+}$ -CaM binds to the cytoplasmic  $\text{NH}_2$ -terminal segment of the rat olfactory channel. (A)  $^{125}\text{I}$ -CaM labeling of membrane proteins obtained from HEK293 cells transfected with different cDNAs (14). Transfection with the olfactory channel cDNA gave an extra CaM-binding protein at about 76-kD compared to transfections with the pCIS expression vector alone or with the rod channel cDNA. Most of the other labeled bands reflect  $\text{Ca}^{2+}$ -CaM-binding proteins endogenous to HEK293 cells. Total protein (100  $\mu\text{g}$ ) was placed in each lane. (B) Experiments on four chimeras (Chi) constructed from rat olfactory and human rod channels. (Top) Putative folding pattern of the olfactory and rod channels in the membrane. CN indicates cyclic nucleotide-binding site. All chimeras have an  $\text{NH}_2$ -terminal region derived from the corresponding region of the olfactory channel and the remainder from the rod channel. The junction points (arrows) are immediately after olfactory channel amino acid (aa) 418 for Chi 38, aa 309 for Chi 140, aa 162 for Chi 1, and aa 139 for Chi 3. (Bottom) Electrical recordings of the effect of  $\text{Ca}^{2+}$ -CaM on homo-oligomeric channels for each chimera; wild-type olfactory and rod channel data are also shown (16). A 60-ms voltage pulse from 0 to  $-60$  mV was delivered every second in the presence of cyclic GMP to monitor the cyclic GMP-induced current. Leakage current was previously subtracted from the recordings. The cyclic GMP concentration was 3  $\mu\text{M}$  for Chi 38 and Chi 140, 10  $\mu\text{M}$  for Chi 1 and Chi 3, 70  $\mu\text{M}$  for the wild-type rod channel and 1.6  $\mu\text{M}$  for the wild-type olfactory channel; none of these cyclic GMP concentrations elicited saturated currents from the respective channels. CaM concentration was 235 nM for Chi 38 and Chi 140, and 250 nM for the other channels. At least three experiments were performed for each channel type, with reproducible results. Solution changes were controlled by solenoid valves and took one to a few seconds to complete in the vicinity of the patch. Dashed line in the solution trace at top indicates region of recording with compressed time course. (C)  $^{125}\text{I}$ -CaM binding to fusion protein containing the cytoplasmic  $\text{NH}_2$ -terminal segment of the olfactory channel, but not to fusion proteins containing the COOH-terminal segment of the olfactory channel or the  $\text{NH}_2$ - or COOH-terminal segments of the rod channel, or to GST. The labeled doublet may reflect some protein degradation. Approximately 10  $\mu\text{g}$  of protein was placed in each lane (17). Bovine brain calmodulin (Sigma, >98 percent purity) was used in all experiments.

can also be recognized in the bovine and fish olfactory channels (Fig. 2A).

**Peptide binding to Ca<sup>2+</sup>-CaM.** In order to quantify the interaction between the binding site and Ca<sup>2+</sup>-CaM, we synthesized a peptide (KY9) corresponding to Arg<sup>62</sup>-Arg<sup>87</sup>. Binding of this peptide to CaM was analyzed with a gel-shift assay, in which a mixture of the peptide and CaM was run on a nondenaturing gel in the presence of Ca<sup>2+</sup> (Fig. 3A). Several ratios of peptide to CaM were used. In the absence of the peptide, there was a single band reflecting pure Ca<sup>2+</sup>-CaM. At a ratio of peptide to CaM of 0.25 or 0.5, two bands were visible on the gel—a Ca<sup>2+</sup>-CaM band and another that migrated with a lower mobility, representing the peptide-Ca<sup>2+</sup>-CaM complex. When the ratio of peptide to CaM was unity, the pure CaM band disappeared and the peptide-CaM complex band concurrently increased in intensity. At still higher ratios, no new bands appeared on the gel, nor did the peptide-Ca<sup>2+</sup>-CaM complex band change in intensity, suggesting that multivalent complexes were absent. These observations suggest that the peptide binds Ca<sup>2+</sup>-CaM with a one-to-one stoichiometry.

By binding to Ca<sup>2+</sup>-CaM, the KY9 peptide is expected to antagonize the modulation of the olfactory channel by Ca<sup>2+</sup>-CaM. Indeed, the steady-state inhibition by Ca<sup>2+</sup>-CaM of a nonsaturating, cyclic GMP-induced current through the channel progressively decreased with increasing concentrations of peptide (Fig. 3B). The inhibition by Ca<sup>2+</sup>-CaM was not observed when the concentration of the peptide exceeded that of CaM, in agreement with one-to-one binding of the peptide to CaM. As controls, two other 26-amino acid peptides (KY8 and KY10) derived from neighboring sequences of the olfactory channel on the NH<sub>2</sub>- and COOH-sides of KY9 failed to antagonize Ca<sup>2+</sup>-CaM action on the channel (Fig. 3C).

The interaction between KY9 and Ca<sup>2+</sup>-CaM was also studied by fluorescence measurements with dansyl-CaM (20). Without the peptide, the photoexcited emission spectrum of dansyl-CaM (300 nM) peaked at 503 nm (Fig. 4A). Addition of 300 nM KY9, which should convert all CaM to the bound form, increased the fluorescence intensity of dansyl-CaM by 1.5 times and shifted the emission peak to about 484 nm. These observations suggest that the dansyl moiety enters a more hydrophobic environment upon binding of the peptide to dansyl-CaM (20). Lower concentrations of the peptide produced intermediate increases in fluorescence and blue shifts. With the dansyl-CaM concentration at 300 nM, the fraction of bound CaM, calculated from the fractional increase in fluorescence intensity (21), increased linearly with total peptide

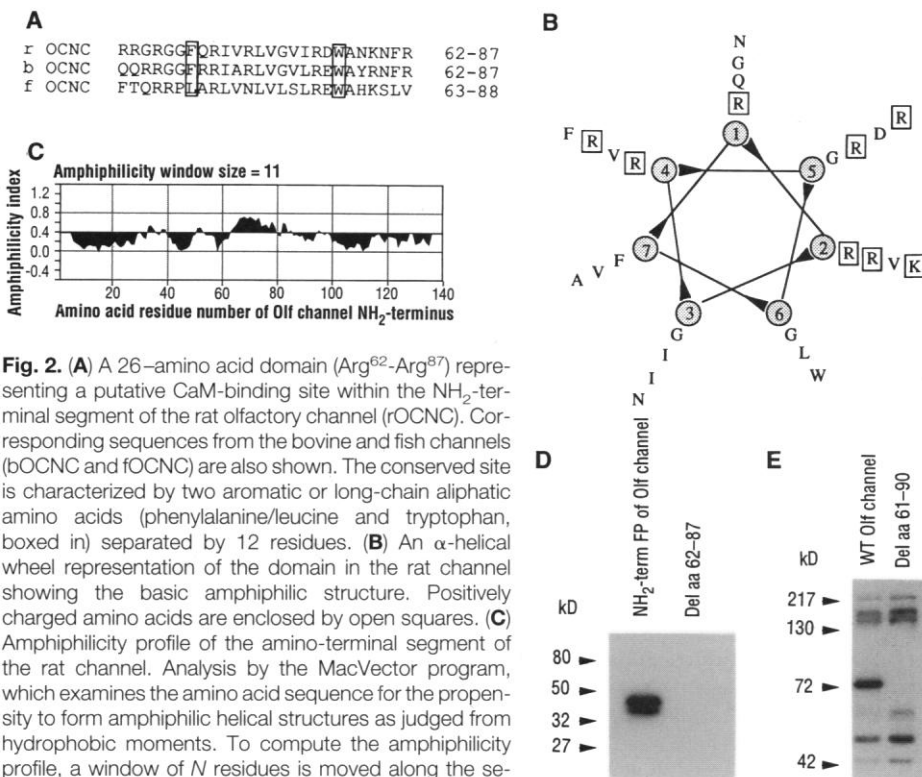


**Fig. 2.** (A) A 26-amino acid domain (Arg<sup>62</sup>-Arg<sup>87</sup>) representing a putative CaM-binding site within the NH<sub>2</sub>-terminal segment of the rat olfactory channel (rOCNC). Corresponding sequences from the bovine and fish channels (bOCNC and fOCNC) are also shown. The conserved site is characterized by two aromatic or long-chain aliphatic amino acids (phenylalanine/leucine and tryptophan, boxed in) separated by 12 residues. (B) An  $\alpha$ -helical wheel representation of the domain in the rat channel showing the basic amphiphilic structure. Positively charged amino acids are enclosed by open squares. (C) Amphiphilicity profile of the amino-terminal segment of the rat channel. Analysis by the MacVector program, which examines the amino acid sequence for the propensity to form amphiphilic helical structures as judged from hydrophobic moments. To compute the amphiphilicity profile, a window of *N* residues is moved along the sequence and centered at one residue at a time; at each window position, the hydrophobic moment is calculated (34). Values greater than about 0.4 indicate amphiphilic regions. In this analysis, *N* = 11 was chosen (34), but a similar profile was obtained with other *N* values such as 20. (D) Deletion of the 26-amino acid domain in (A) from the olfactory channel NH<sub>2</sub>-terminal fusion protein abolished CaM binding, as assayed with <sup>125</sup>I-CaM. Deletion mutagenesis of double-stranded DNA was performed with the U.S.E. (unique site elimination) mutagenesis kit from Pharmacia. (E) Deletion of a region containing the same 26-amino acid domain from the whole olfactory channel protein (same as Del 86 in Fig. 5) likewise abolished CaM binding (again assayed with <sup>125</sup>I-CaM), indicating that this domain represents the only CaM-binding site on the protein. Deletion mutagenesis was performed on single-stranded DNA.

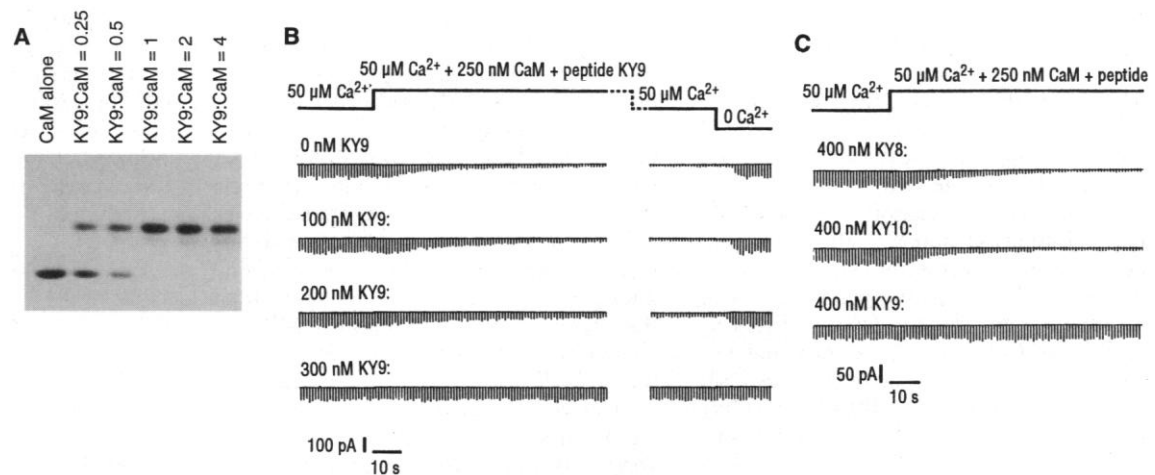
concentration until the signal saturated at equimolar concentrations of dansyl-CaM and peptide (Fig. 4B). These data suggested a dissociation constant between the peptide and CaM that is considerably lower than 300 nM and at the same time confirmed one-to-one binding between the two. To measure this dissociation constant, we reduced the dansyl-CaM concentration to about 3 nM and plotted the fraction of bound dansyl-CaM as a function of free peptide concentration. Data from two experiments led to a dissociation constant of about 3.4 nM (Fig. 4C).

As pointed out earlier, the CaM-binding site in the NH<sub>2</sub>-terminal segment of the rat olfactory channel appears to be also present in the fish channel (Fig. 2A). To verify the site in the fish channel, we synthesized another peptide corresponding to its sequence and confirmed binding of the peptide to Ca<sup>2+</sup>-CaM by means of the gel-shift assay. This observation is consistent with the previous finding that the fish channel is also modulated by CaM (6). Thus, this modulation appears to be common among vertebrates, supporting its essential role in

olfactory adaptation (6).

**Mechanism of Ca<sup>2+</sup>-CaM modulation and involvement of the NH<sub>2</sub>-terminal segment in channel gating.** To investigate the mechanism underlying the CaM-induced decrease in apparent affinity of the olfactory channel for cyclic nucleotide, we divided the cytoplasmic NH<sub>2</sub>-terminal segment of the olfactory channel into five regions of 30 amino acids each and measured by electrophysiological means the effect of deleting each region. One deletion mutant, Del 85, behaved like the wild-type channel (Fig. 5A); thus, half-activation of the channel in control conditions occurred at a cyclic GMP concentration (*K*<sub>1/2</sub>) of 2.8  $\mu$ M, and in the presence of 50  $\mu$ M Ca<sup>2+</sup> and 250 nM CaM the *K*<sub>1/2</sub> became 14.3  $\mu$ M (compare Fig. 6A). Also like the wild type, CaM produced no obvious change in the maximum current. For another mutant, Del 86, for which the deleted region contained the CaM-binding domain, the control cyclic GMP dose-response relation was shifted to a position near that for the wild-type channel in the presence of Ca<sup>2+</sup>-CaM, and Ca<sup>2+</sup>-CaM had no effect (Fig. 5B). In ad-

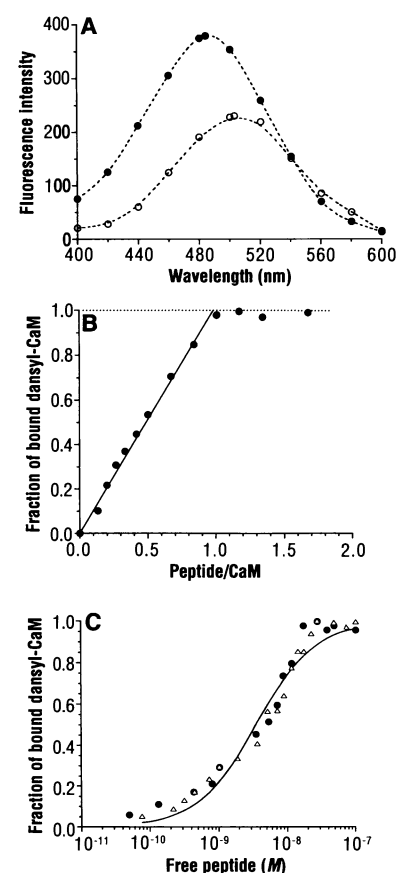
**Fig. 3.** Interaction between olfactory channel Arg<sup>62</sup>-Arg<sup>87</sup> peptide (KY9) and Ca<sup>2+</sup>-CaM. **(A)** Binding of the peptide to Ca<sup>2+</sup>-CaM studied in a gel mobility-shift assay. KY9, with sequence corresponding to the 26-amino acid domain in Fig. 2A, was synthesized on an Applied Biosystems peptide synthesizer and purified by reversed-phase high-performance liquid chromatography (HPLC). Mixtures of peptide and CaM at different molar ratios (with CaM concentration fixed at 1 nM) were incubated in 10 mM sodium-Hepes, pH 7.2, and 1 mM CaCl<sub>2</sub> for 30 minutes at room temperature. A portion (25  $\mu$ l) of each mixture was then separated by nondenaturing polyacrylamide gel electrophoresis in the presence of 1 mM Ca<sup>2+</sup>. Being negatively charged, CaM migrated toward the positive pole in the bottom of the gel (lane 1). The complex formed (in lanes 2 to 6) between the peptide and Ca<sup>2+</sup>-CaM was stable during electrophoresis and migrated with a lower mobility because of positive charges on the peptide and a higher molecular mass of the complex (Coomassie blue stain). Removal of Ca<sup>2+</sup> by EGTA in a control experiment abolished complex formation. **(B)** KY9 blocked the modulation of the wild-type olfactory channel by CaM. All traces from the same patch. Experimental procedures were the same as in Fig. 1B; the peptide was added



together with CaM. Cyclic GMP concentration was 1.6  $\mu$ M, which did not saturate the current. Three patches gave the same results. **(C)** Comparison of the abilities of three olfactory channel peptides, KY8, KY9, and KY10, to block the CaM modulation of the olfactory channel. The sequence of KY8 is NHHPPPSIKANGKDDHRAGSRPQSV (residues 18 to 43), which is NH<sub>2</sub>-terminal of KY9; the sequence of KY10 is PRPDSFLERFRGPELQTVT-THQGDDK (residues 91 to 116), which is COOH-terminal of KY9. Only KY9 blocked the CaM modulation. All traces from the same patch. Same experimental conditions as in (B). Two patches gave the same results. Abbreviations for the amino acid residues are: A, Ala; C, Cys; D, Asp; E, Glu; F, Phe; G, Gly; H, His; I, Ile; K, Lys; L, Leu; M, Met; N, Asn; P, Pro; Q, Gln; R, Arg; S, Ser; T, Thr; V, Val; W, Trp; and Y, Tyr.

dition to the above five mutants, others were constructed and tested, with the overall results summarized in Fig. 5C. These results suggest the presence of a domain in the NH<sub>2</sub>-terminal segment of the olfactory channel that contributes to the high apparent affinity of the channel for ligand. If this domain is deleted, or when Ca<sup>2+</sup>-CaM binds to the vicinity in the wild-type channel and "blocks" its influence, the apparent affinity of the channel for ligand decreases. This domain begins at around Pro<sup>61</sup>, but its COOH-terminal border is still undefined because of the inability to test some of the mutants (see Fig. 5C legend). The question remains as to how the NH<sub>2</sub>-terminal domain of the olfactory channel contributes to the high apparent ligand affinity. Because the current through the wild-type channel at high concentrations of cyclic GMP is unchanged by Ca<sup>2+</sup>-CaM (Fig. 6A) (6), it might be proposed that the modulation involves only the ligand-binding step. However, experiments with cyclic GMP as the ligand indicate that this is not the case. Along with the increase in adenosine 3',5-monophosphate (cyclic AMP)  $K_{1/2}$  that is due to Ca<sup>2+</sup>-CaM, there is also a substantial decrease in the maximum cyclic AMP-induced current (Fig. 6B) (6). Because the single-channel current induced by cyclic AMP is not affected by Ca<sup>2+</sup>-CaM (6), the reduction in macroscopic current at saturating cyclic AMP concentrations must reflect a change in the opening probability of the channel, that is,

**Fig. 4.** Fluorescence measurement of the interaction between peptide KY9 and CaM. **(A)** Emission fluorescence spectra of dansyl-CaM with and without KY9. Open circles, 300 nM dansyl-CaM in a buffer containing 50 mM tris-Cl, pH 7.3, 150 mM NaCl, and 0.5 mM CaCl<sub>2</sub>. Filled circles, 300 nM CaM plus 300 nM KY9 peptide in the same buffer. Emission fluorescence (arbitrary units) was measured with a Shimadzu RF-1501 spectrofluorometer; excitation wavelength was at 340 nm. Both excitation and emission band-passes were 10 nm. The spectra were corrected for background buffer fluorescence. Dashed curves were fitted by eye. **(B)** Fraction of bound dansyl-CaM as a function of added peptide concentration. The buffer was the same as in (A) containing 300 nM dansyl-CaM, into which portions of a concentrated peptide solution were sequentially added; the resulting dilution of the original CaM solution was less than 1 percent. The fraction of bound CaM was calculated from the fractional fluorescence increase at 480 nm (27). The solid line indicates a linear relation between bound CaM and added peptide until all CaM became bound (and the signal saturated) at a molar ratio of one between peptide and CaM. **(C)** Determination of the dissociation constant between KY9 peptide and CaM. Same procedures as in (B), except concentration of dansyl-CaM in the buffer was 3.3 nM. Data from two experiments are shown. The free peptide concentration plotted on the abscissa was obtained by subtracting the peptide-CaM complex concentration (calculated as the product of the fractional fluorescence increase and the total CaM concentration of 3.3 nM) from the total added peptide concentration. The curve is a least-squares fit of the Hill equation, with a Hill coefficient of 1.02 and a dissociation constant of 3.4 nM.



a modulation of the gating step.

To examine whether a change in channel gating alone can account for the shift in

apparent affinity, we have adopted the following empirical model for the operation of this channel

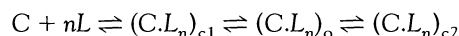


where  $C$  is the channel,  $L$  is cyclic nucleotide,  $(C.L_n)_c$  and  $(C.L_n)_o$  are the closed and open states of the liganded channel, respectively,  $n$  is the Hill coefficient,  $K_d$  is the "effective" dissociation constant of the binding step (22), and  $K_g$  is the probability ratio of the channel in the open and closed states (that is, the gating parameter). The open probability,  $P_o$ , is related to  $K_g$  by  $P_o = K_g/(1 + K_g)$ . It can be shown that the current activated by cyclic nucleotide,  $I(L)$ , is proportional to  $[K_g/(1 + K_g)]L^n/(L^n + K_{1/2}^n)$ , where  $L$  here is ligand concentration and  $K_{1/2} = K_d/(1 + K_g)^{1/n}$ . The relation between  $K_{1/2}$  and  $K_g$  embodies the effect of channel gating on the apparent ligand affinity. The effects of CaM on the cyclic GMP and cyclic AMP dose-response relations can both be fit by curves derived from this model (see legend for parameter values), with the gating parameter  $K_g$  taken to be the only parameter affected (decreased) by  $Ca^{2+}$ -CaM (Fig. 6, A and B). Briefly, the key assumption is that, in the absence of  $Ca^{2+}$ -CaM, the channel has a  $P_o$  approaching unity (that is, permanently open) when cyclic GMP is bound. In other words,  $K_g$  is very large, such that  $P_o$  is little affected even when  $K_g$  is decreased more than 100 times by  $Ca^{2+}$ -CaM, thus explaining the constancy of maximum current; in contrast, the  $K_{1/2}$  will increase by an order of magnitude with  $Ca^{2+}$ -CaM, as observed. For cyclic AMP,  $K_g$  is also high, but not as high as for cyclic GMP, so that while  $P_o$  is near unity in the control condition [hence the nearly identical saturated currents elicited by cyclic GMP and cyclic AMP as described in (10)], a 100-fold reduction in  $K_g$  by  $Ca^{2+}$ -CaM will decrease  $P_o$  substantially below unity, explaining the observed concomitant reduction in saturated current and increase in  $K_{1/2}$ . The deletion mutants described above showed behaviors in response to cyclic AMP that likewise could be predicted from their behaviors in response to cyclic GMP. For example, Del 129, which behaved like the wild-type channel with cyclic GMP as ligand (Fig. 5C), also yielded a control cyclic AMP dose-response relation like that of the wild type (Fig. 6C). In contrast, Del 86, which showed a control cyclic GMP dose-response relation already shifted to a position close to that for the wild-type channel with  $Ca^{2+}$ -CaM, also showed a shifted cyclic AMP dose-response relation and a reduced  $P_o$  (reflected by the substantially smaller current produced by cyclic AMP than by cyclic GMP) even without  $Ca^{2+}$ -CaM (Fig. 6D). These observations suggest that, for both cyclic GMP and cyclic AMP as ligand, deletion of a key domain in the  $NH_2$ -terminal segment is

equivalent to the binding of  $Ca^{2+}$ -CaM to the wild-type channel, justifying the above analysis based on a comparison of cyclic GMP and cyclic AMP results.

The assumption that the  $P_o$  of the channel in the absence of  $Ca^{2+}$ -CaM is near unity can only be verified with membrane patches containing a single expressed channel. Because the olfactory channel exhibits high expression in HEK293 cells, only one such patch was encountered (Fig. 6E). In the presence of 30  $\mu$ M cyclic GMP, the channel indeed stayed largely in the open state. The  $P_o$  value estimated from 12 traces such as those shown in Fig. 6E was 0.94 (after a minor correction to  $-60$  mV, the voltage used in all dose-response relations). This value is near unity, although perhaps not quite high enough to fully support the above calculations (which require a  $P_o \approx 1.0$  for cyclic GMP). The measured  $P_o$  might increase slightly if the cyclic GMP concentration were higher than 30  $\mu$ M, a concentration that is not fully saturating.

The  $P_o$  would certainly approach unity, however, if infrequent long closures (one example is shown in Fig. 6E) were discounted. These infrequent long closures appear to represent a second closed state of the fully liganded channel (23, 24); that is, the kinetic scheme is better represented by



where  $(C.L_n)_{c2}$  represents the long, closed state. From this scheme, the presence of the long, closed state actually favors ligand binding to the channel and hence should be grouped with the open state  $(C.L_n)_o$  for  $P_o$  calculations, making it practically equal one. In summary, the observed change in ligand affinity of the channel due to  $Ca^{2+}$ -CaM can be explained by an effect on the gating step.

**Comparisons.** Our experiments indicate that  $Ca^{2+}$ -CaM modulates the olfactory cyclic nucleotide-activated channel by directly binding to it, dramatically reducing its apparent affinity for cyclic nucleotide as

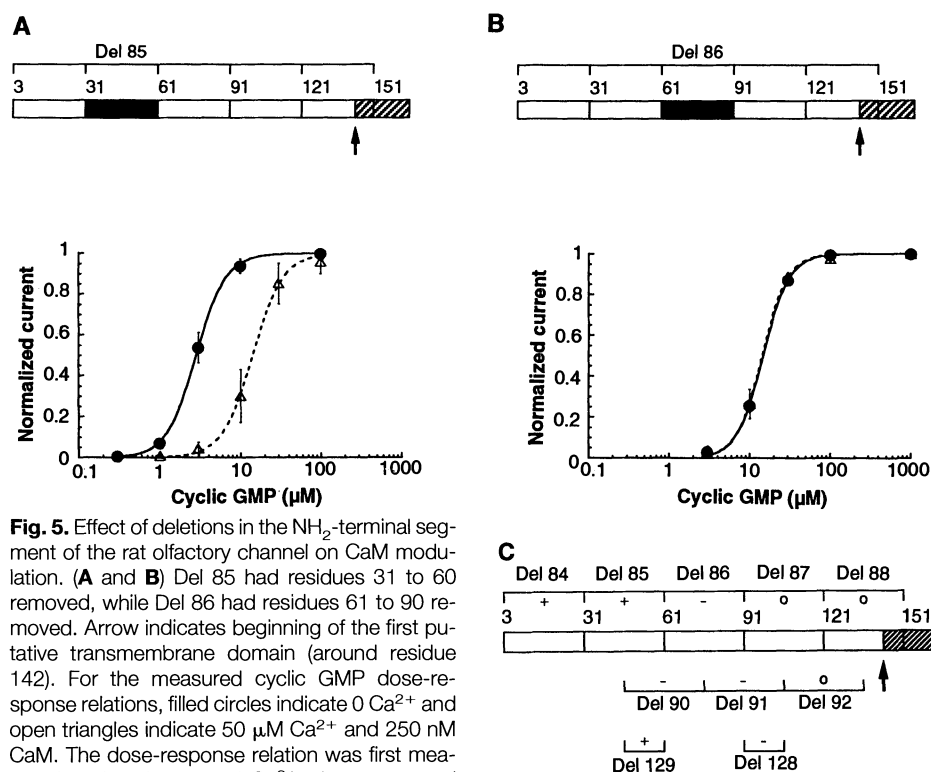


**Fig. 5.** Effect of deletions in the  $NH_2$ -terminal segment of the rat olfactory channel on CaM modulation. **(A and B)** Del 85 had residues 31 to 60 removed, while Del 86 had residues 61 to 90 removed. Arrow indicates beginning of the first putative transmembrane domain (around residue 142). For the measured cyclic GMP dose-response relations, filled circles indicate 0  $Ca^{2+}$  and open triangles indicate 50  $\mu$ M  $Ca^{2+}$  and 250 nM CaM. The dose-response relation was first measured in the absence of  $Ca^{2+}$ , then measured again after the patch was perfused with  $Ca^{2+}$ -CaM solution for 1 minute. All currents were measured at  $-60$  mV and normalized against the value in the absence of  $Ca^{2+}$  at 100  $\mu$ M cyclic GMP for Del 85 and 1000  $\mu$ M cyclic GMP for Del 86. The points represent averaged measurements from three patches for Del 85 and 5 patches for Del 86; error bars are standard deviations. Curves are from the Hill equation,  $I_{norm} = C^n / [C^n + K_{1/2}^n]$ , where  $I_{norm}$  is normalized current,  $C$  is cyclic GMP concentration, and  $n$  is Hill coefficient. For Del 85, the  $K_{1/2}$  and  $n$  values are 2.8  $\mu$ M, 2.4 in the absence of  $Ca^{2+}$  and 14.3  $\mu$ M, 2.3 with  $Ca^{2+}$ -CaM. For Del 86, the corresponding values are 14.8  $\mu$ M, 2.7 in the absence of  $Ca^{2+}$  and 14.4  $\mu$ M, 2.8 with  $Ca^{2+}$ -CaM. **(C)** Overall results from ten deletion mutants. Del 90–92 had deletions displaced by 15 amino acids from those for Del 85–87. Del 128 and Del 129 consisted of deletions of the overlapping regions between Del 85 and Del 90, and Del 87 and Del 91, respectively. +, the mutant behaved like wild type. –, the control behavior of the mutant was like wild type with  $Ca^{2+}$ -CaM; furthermore,  $Ca^{2+}$ -CaM had no effect. 0, the mutant showed either low or no obvious functional expression, precluding proper testing.

a result. The mechanism underlying this modulation is similar to the control mechanisms for CaM-regulated enzymes. For example, in the case of CaM kinase II, there is an autoinhibitory domain in the molecule that normally prevents catalytic activity of the enzyme; when  $\text{Ca}^{2+}$ -CaM binds to an overlapping domain, however, the influence of the inhibitory domain is removed, thereby activating the enzyme (25). A similar mechanism involving disinhibition is thought to underlie the CaM activation of other enzymes such as myosin light chain kinase, calcineurin, and CaM-phosphodiesterase (25). The same applies to the  $\text{Ca}^{2+}$ -adenosine triphosphatase and the  $\text{Na}^+$ - $\text{H}^+$  exchanger (26).

In the case of the olfactory channel, CaM does not "activate" the channel; in fact, the likelihood of the channel being activated by ligand is reduced by CaM. Nonetheless, the modulatory mechanism still involves the displacement or blockage of an intrinsically active domain in the target protein by CaM. Apart from the olfactory channel, several other ion channels also appear to be directly gated or modulated by  $\text{Ca}^{2+}$ -CaM (2–5, 27), but their CaM-binding sites remain to be identified, as do the underlying mechanisms. Nonetheless, indirect evidence from limited proteolysis experiments suggests that at least the activation by  $\text{Ca}^{2+}$ -CaM of the  $\text{Ca}^{2+}$ -dependent  $\text{K}^+$  channel in *Parameci-*

*um* and a  $\text{K}^+$  channel in kidney medulla may also be through a disinhibitory mechanism (2, 4). Because  $\text{Ca}^{2+}$  is a common intracellular messenger and CaM is nearly ubiquitous in cells, a direct  $\text{Ca}^{2+}$ -CaM modulation of ion channels may be more widespread than has been realized.

The CaM-binding site of the olfactory channel exhibits features characteristic of other CaM-binding sites, including the presence of two aromatic or "long-chain" aliphatic amino acids (Phe<sup>68</sup> and Trp<sup>81</sup>) separated by 12 residues and the tendency to form a basic amphiphilic  $\alpha$  helix (18, 19). To examine this site a little further, we synthesized another peptide that had only 18 residues (Arg<sup>62</sup>-Arg<sup>79</sup>), purposely avoiding the tryptophan residue in position 81. This peptide still bound  $\text{Ca}^{2+}$ -CaM. It is possible that CaM does interact strongly with Trp<sup>81</sup> in the native channel, but in the absence of this residue  $\text{Ca}^{2+}$ -CaM can also interact with perhaps Ile<sup>78</sup> (another "long-chain" aliphatic amino acid) as a substitute. From x-ray structures, the interaction between CaM and the binding site on CaM kinase II appears to involve two key hydrophobic amino acids separated by only eight residues (28). These observations underscore the flexibility in the interaction between CaM and its target site, attributed to the compliance of the central helix linking the two globular lobes (18, 28, 29).

Finally, the experiments with cyclic AMP as ligand indicate that  $\text{Ca}^{2+}$ -CaM affects channel gating, in that the current activated by high cyclic AMP concentrations is significantly reduced by  $\text{Ca}^{2+}$ -CaM. Furthermore, our simple kinetic analysis suggests that this effect on channel gating is sufficient to account for the observed change in apparent ligand affinity. A concomitant effect by  $\text{Ca}^{2+}$ -CaM on the ligand-binding step cannot be ruled out, but is unnecessary for explaining the observations. In general, it is difficult to completely separate contributions from the ligand-binding and the gating steps because the two are tightly coupled (30). The kinetic model we have adopted for analysis is empirical. However, a more realistic model with independent binding sites (24) or a Monod-Wyman-Changeux-type allosteric scheme (31) would also lead to the same conclusion (22). The finding that the  $\text{NH}_2$ -terminal segment of the olfactory channel contributes to the gating process is unexpected, considering that the cyclic nucleotide-binding site is located in the  $\text{COOH}$ -terminal segment. Since cyclic nucleotide-gated cation channels share structural homology with voltage-activated  $\text{K}^+$  channels, and to a lesser degree also other voltage-gated channels, this property may conceivably exist in these other channels as well.

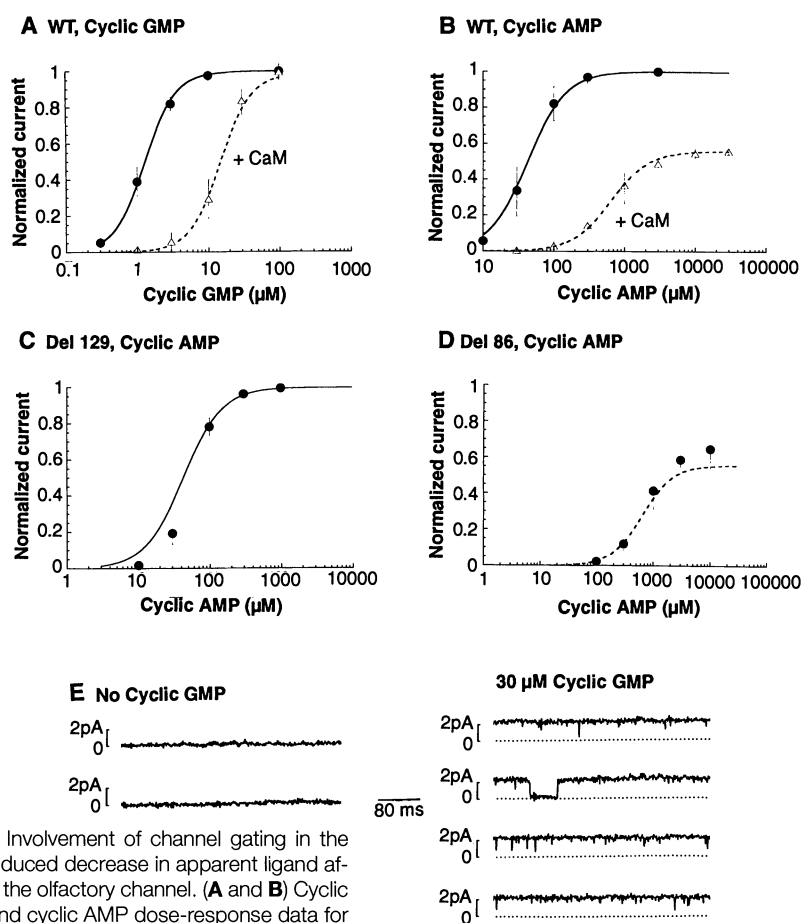


**Fig. 6.** Involvement of channel gating in the CaM-induced decrease in apparent ligand affinity of the olfactory channel. (**A** and **B**) Cyclic GMP and cyclic AMP dose-response data for the wild-type olfactory channel adapted from Chen and Yau (6). Smooth curves are drawn according to  $I(L) = [K_g / (1 + K_g)] [L^n / (L^n + K_{1/2}^n)]$ , where  $K_{1/2} = K_g / (1 + K_g)^{1/n}$ . For cyclic GMP,  $K_g = 121 \mu\text{M}$ ,  $n = 2$ ;  $K_g = 8650$  in  $0 \text{ Ca}^{2+}$  and  $67.6$  in  $\text{Ca}^{2+}$ -CaM. For cyclic AMP,  $K_g = 1077 \mu\text{M}$ ,  $n = 1.6$ ,  $K_g = 173$  in  $0 \text{ Ca}^{2+}$  and  $1.27$  in  $\text{Ca}^{2+}$ -CaM. From these parameters, it can be calculated that  $P_o = 1.0$ ,  $K_{1/2} = 1.3 \mu\text{M}$  in  $0 \text{ Ca}^{2+}$  and  $P_o = 0.985$ ,  $K_{1/2} = 14.6 \mu\text{M}$  in  $\text{Ca}^{2+}$ -CaM for cyclic GMP, and  $P_o = 0.994$ ,  $K_{1/2} = 43 \mu\text{M}$  in  $0 \text{ Ca}^{2+}$  and  $P_o = 0.56$ ,  $K_{1/2} = 645 \mu\text{M}$  in  $\text{Ca}^{2+}$ -CaM for cyclic AMP. (**C**) Cyclic AMP dose-response relation obtained from Del 129, with maximum current normalized with respect to that produced by cyclic GMP. Curve is identical to the solid curve in (**B**) in both form and position. (**D**) Cyclic AMP dose-response relation obtained from Del 86. Curve is identical to the dashed curve in (**B**) in both form and position. (**E**) Recordings from the only single-channel patch encountered for the expressed wild-type olfactory channel. (Left) Sample traces in the absence of cyclic GMP. (Right) Sample traces in the presence of  $30 \mu\text{M}$  cyclic GMP. Zero- $\text{Ca}^{2+}$  solution on both sides of the membrane. The liganded channel was literally always open, except for the infrequent long closures. Membrane potential was at  $+60 \text{ mV}$ . The  $P_o$  measured from 12 traces was  $0.96$ . From the macroscopic current-voltage relation previously measured under the same conditions (10), the corresponding  $P_o$  at  $-60 \text{ mV}$  would be about  $0.94$ .

## REFERENCES AND NOTES

1. L. K. Kaczmarek and I. B. Levitan, *Neuromodulation: The Biochemical Control of Neuronal Excitability* (Oxford Univ. Press, New York, 1987); B. Hille, *Ionic Channels of Excitable Membranes* (Sinauer, Sunderland, MA, ed. 2, 1992); I. B. Levitan, *Annu. Rev. Physiol.* **56**, 193 (1994).
2. Y. Saimi and K.-Y. Ling, *Science* **249**, 1441 (1990); A. Kubalski, B. Martinac, Y. Saimi, *J. Membrane Biol.* **112**, 91 (1989); Y. Saimi, K.-Y. Ling, C. Kung, in *Handbook of Membrane Channels: Molecular and Cellular Physiology*, C. Peracchia, Ed. (Academic, New York, 1993), pp. 435–443.
3. J. S. Smith, E. Rousseau, G. Meissner, *Circulation Res.* **64**, 352 (1989).
4. D. A. Klaerke, S. J. D. Karlsh, P. L. Jorgensen, *J. Membrane Biol.* **95**, 105 (1987); D. A. Klaerke, J. Petersen, P. L. Jorgensen, *FEBS Lett.* **216**, 211 (1987).
5. T.-Y. Chen *et al.* *Proc. Natl. Acad. Sci. U.S.A.* **91**, 11757 (1994); Y.-T. Hsu and R. S. Molday, *Nature* **361**, 76 (1993).
6. T.-Y. Chen and K.-W. Yau, *Nature* **368**, 545 (1994).
7. T. Kurahashi and T. Shibuya, *Brain Res.* **515**, 261 (1990).
8. R. H. Kramer and S. A. Siegelbaum, *Neuron* **9**, 897 (1992).
9. U. B. Kaupp *et al.*, *Nature* **342**, 762 (1989); W. Bönick *et al.*, *Neuron* **10**, 865 (1993); J. Ludwig, T. Margalit, E. Eismann, D. Lancet, U. B. Kaupp, *FEBS Lett.* **270**, 24 (1990); E. H. Gouling *et al.*, *Neuron* **8**, 45 (1992).
10. R. S. Dhallan, K.-W. Yau, K. A. Schrader, R. R. Reed, *Nature* **347**, 184 (1990).
11. L.-Y. Jan and Y. N. Jan, *Nature* **345**, 672 (1990); H. R. Guy, S. R. Durell, J. Warmke, R. Drysdale, B. Ganetzky, *Science* **254**, 730 (1991); L. Heginbotham, T. Abramson, R. MacKinnon, *ibid.* **258**, 1152 (1992); E. H. Gouling, G. R. Tibbs, D. Liu, S. A. Siegelbaum, *Nature* **364**, 61 (1993).
12. T.-Y. Chen *et al.*, *Nature* **362**, 764 (1993).
13. J. Bradley, J. Li, N. Davidson, H. Lester, K. Zinn, *Proc. Natl. Acad. Sci. U.S.A.* **91**, 8890 (1994); E. R. Liman and L. B. Buck, *Neuron* **13**, 611 (1994).
14. The cDNAs encoding the rat olfactory and human rod channels were inserted into a pCIS expression vector containing a cytomegalovirus (CMV) promoter. The construct RSV-Tag contains the SV40 T antigen under the control of the Rous sarcoma virus (RSV) promoter. Procedures for transient transfection of the cDNAs into HEK293 cells have been described (10). At 48 to 72 hours after transfection, the cells were lysed and the membrane fraction was centrifuged. The pellet was then solubilized, separated by SDS-PAGE, and transferred onto a nitrocellulose membrane. The nonspecific sites on the membrane were blocked by a buffer containing 10 mM imidazole, pH 7.4, 150 mM KCl, 1 mM CaCl<sub>2</sub>, 0.2 percent Tween 20, and 5 percent bovine serum albumin (BSA) or dry milk. <sup>125</sup>I-labeled bovine CaM (NEN, final activity of 5 × 10<sup>6</sup> cpm/ml) was overlaid on the membrane for 4 to 5 hours at room temperature. The membrane was washed extensively in the above buffer without BSA or milk. CaM-binding proteins were detected by autoradiography.
15. A tandem construct consisting of olfactory channel cDNA at the 5' end and rod channel cDNA at the 3' end separated by a unique restriction site was subcloned into pBluescript. After linearization at the restriction site, the plasmid was transformed into *Escherichia coli* HB101 cells, where an unknown *in vivo* mechanism resulted in many different chimeric recombinants (R. R. Reed and L. R. Levin, personal communication). The chimeras were screened by restriction mapping and sequencing.
16. Electrical recordings on inside-out membrane patches excised from transfected HEK293 cells were carried out 48 to 72 hours after transfection with an Axopatch 1D patch-clamp amplifier at bandwidth DC-1 KHz. The signals were either recorded on a tape recorder or digitized directly onto a computer for measuring current amplitude. The recording pipettes were fabricated from borosilicate glass and had tip lumen diameters of about 1 μm. Seal resistances of the excised membrane patches were 2 to 10 Gohm. The pipette contained "0 Ca<sup>2+</sup>" solution with 140 mM NaCl, 5 mM KCl, 1 mM sodium-EGTA, 10 mM sodium-Hepes, pH 7.4. The bath contained either "0 Ca<sup>2+</sup>" solution, or 50 μM free Ca<sup>2+</sup> solution that had the same composition but with 704 μM CaCl<sub>2</sub> and 2 mM sodium nitrilotriacetic acid present instead of sodium-EGTA to give the correct buffered Ca<sup>2+</sup> concentration. Appropriate concentrations of cyclic GMP were added to the bath solution. Experiments were performed at room temperature.
17. Fusion proteins composed of GST and the NH<sub>2</sub>- or COOH-terminal segments of the rat olfactory and human rod channels were constructed in pGEX-2T plasmid (Pharmacia). The NH<sub>2</sub>- and COOH-terminal sequences of the olfactory channel spanned amino acids 1 to 131 and 380 to 664, respectively, while those of the rod channel spanned amino acids 1 to 156 and 391 to 686, respectively. The coding sequences were obtained by the polymerase chain reaction (PCR), in which appropriate pairs of oligonucleotide primers with flanking Bam HI and Eco RI restriction sites were used. The PCR products were subcloned in frame into pGEX-2T and then transformed into *E. coli* BL21 cells. The production of fusion protein was essentially as described (32). Briefly, after the overnight cultures had grown to mid-log phase in 2 × YT media, up to 0.2 mM of isopropyl β-D-thiogalactopyranoside (IPTG) was added to induce the production of fusion protein. Cells were centrifuged and resuspended in a lysis buffer consisting of 20 mM sodium-HEPES, pH 7.4, 100 mM KCl, 1 mM EDTA, 1 mM dithiothreitol (DDT), 1 mM phenylmethylsulfonyl fluoride (PMSF), aprotinin at 10 μg/ml, leupeptin at 10 μg/ml, and pepstatin at 10 μg/ml. The cells were lysed on ice with a probe sonicator. The fusion protein was solubilized with 1 percent Triton X-100 and 1 percent CHAPS, purified with glutathione-agarose beads (1:1 slurry) or on a column, and eluted with a buffer containing 20 mM Tris-Cl, pH 7.4, and 10 mM reduced glutathione.
18. M. Ikura *et al.*, *Science* **256**, 632 (1992).
19. K. T. O'Neil and W. F. DeGrado, *Trends Biochem.* **15**, 59 (1990).
20. R. L. Kincaid, M. Vaughan, J. C. Osborne Jr., V. A. Tkachuk, *J. Biol. Chem.* **257**, 10638 (1982); H. Munnier *et al.*, *FEBS Lett.* **190**, 409 (1991); B. Bertrand, S. Wakabayashi, T. Ikeda, J. Pouyssegur, M. Shigekawa, *J. Biol. Chem.* **269**, 13703 (1994).
21. For an arbitrary ratio of free and liganded dansyl-CaM in a binary mixture, the emission fluorescence at any wavelength is given by a linear combination of the separate fluorescence from the two species. At a given wavelength, let  $I_f$  be the fluorescence if all dansyl-CaM is free,  $I_b$  be the fluorescence if all dansyl-CaM is bound to the peptide, and  $I_m$  be the measured fluorescence for any intermediate mixture of the two. Then, if  $f_b$  represents the fraction of bound CaM, we have  $I_m = I_f(1 - f_b) + I_b f_b$ . Rearranging terms, we get  $f_b = (I_m - I_f)/(I_b - I_f)$ . That is, the fraction of bound dansyl-CaM is simply the fractional increase in fluorescence. Our measurements were made at 480 nm.
22. Consider the following kinetic scheme for the olfactory channel with  $n$  cyclic nucleotide-binding sites:  $C \rightleftharpoons C.L \rightleftharpoons C.L_2 \rightleftharpoons \dots \rightleftharpoons C.L_n \rightleftharpoons (C.L_n)_o$ , where C is the channel, L is cyclic nucleotide, and  $(C.L_n)_o$  is the open state. The dissociation constants for the sites,  $K_1, K_2, \dots, K_n$ , are given by  $K_1 = k_{-1}/k_1, K_2 = k_{-2}/k_2, \dots, K_n = k_{-n}/k_n$ , where  $k_1, k_2, \dots, k_n$  and  $k_{-1}, k_{-2}, \dots, k_{-n}$  are the ligand on and off rates, respectively. In the limiting case of infinite cooperativity between the binding sites (that is, ligand binding to one site promotes "simultaneous" ligand binding to the other sites, and likewise for the unbinding step), the kinetic scheme reduces to that shown in the text, with  $K_d$  representing the "effective" dissociation constant, defined as  $K_d = (K_1 K_2 \dots K_n)^{1/n}$ . By analogy to the voltage-activated Shaker-type K<sup>+</sup> channel (33), this channel is likely to be a tetramer so that there should be four binding sites for cyclic nucleotide. Thus, in principle, we have  $n=4$ . The fact that the observed Hill coefficient for the cyclic nucleotide dose-response relation is only about 2 (6, 10) suggests that the above model is oversimplified. However, as an empirical model it is useful because there are only two parameters,  $K_d$  and  $K_g$ . We have adopted this model and taken the  $n$  value to equal the observed Hill coefficient. A more realistic model would be to assume independent binding to the  $n$  identical sites (24). In this case, it can be shown that  $I(L) \propto K_d / (1 + K_d/L)^n + K_g$ , where  $K_d$  here is the microscopic dissociation constant of each site. However, with  $n = 4$ , even this form will not fit the experimental dose-response relation very well, especially for large  $K_g$  (24) because the predicted Hill coefficient would still be too large. This discrepancy can be eliminated if we assume that the channel can open without all of the sites being occupied. In this case, however, an even more general model would be the Monod-Wyman-Changeux allosteric model (31), in which the channel even without ligand has a finite probability of being open, and this open probability progressively increases with an increasing number of cyclic nucleotide molecules bound. We have not adopted this kind of model for our analysis because it involves more free parameters than the empirical Hill equation model described above. Nevertheless, the overall conclusion regarding the effect of gating on ligand binding would not be affected by the choice of model.
23. G. Matthews and S.-I. Watanabe, *J. Physiol. (London)* **403**, 389 (1988).
24. L. W. Haynes and K.-W. Yau, *ibid.* **429**, 451 (1990).
25. T. R. Soderling, *J. Biol. Chem.* **265**, 1823 (1990); A. R. Means, *Recent Prog. Hormone Res.* **44**, 223 (1988); M. H. Krinks, J. Haiech, A. Rhoads, C. B. Klee, *Adv. Cyclic Nucleotide Protein Phosph. Res.* **18**, 31 (1984); H. W. Jarrett and R. Madhavan, *J. Biol. Chem.* **266**, 362 (1991).
26. A. Enyedi *et al.*, *J. Biol. Chem.* **264**, 12313 (1989); R. Falchetto, T. Vorherr, J. Brunner, E. Carafoli, *ibid.* **266**, 2930 (1991); S. Wakabayashi, B. Bertrand, T. Ikeda, J. Pouyssegur, M. Shigekawa, *ibid.* **269**, 13710 (1994).
27. A. M. Phillips, A. Bull, L. E. Kelly, *Neuron* **8**, 631 (1992); R. C. Hardie and B. Minke, *ibid.*, p 643; Y. Hu *et al.*, *Biochem. Biophys. Res. Commun.* **201**, 1050 (1994).
28. W. E. Meador, A. R. Means, F. A. Quiocho, *Science* **262**, 1718 (1993).
29. M. F. A. VanBerkum, S. E. George, A. R. Means, *J. Biol. Chem.* **265**, 3750 (1990).
30. D. Colquhoun and M. Farrant, *Nature* **366**, 510 (1993).
31. L. Stryer, *Chem. Scripta* **27B**, 161 (1987).
32. D. B. Smith and K. S. Johnson, *Gene* **67**, 31 (1988).
33. R. MacKinnon, *Nature* **350**, 232 (1991); M. Li, N. Unwin, K. A. Stauffer, Y.-N. Jan, L. Y. Jan, *Current Biol.* **4**, 110 (1994).
34. D. Eisenberg, R. M. Weiss, T. C. Terwilliger, *Proc. Natl. Acad. Sci. U.S.A.* **81**, 140 (1984); D. Eisenberg, E. Schwarz, M. Komaromy, R. Wall, *J. Mol. Biol.* **179**, 125 (1984).
35. We thank J. Finn, R.-C. Huang, R. L. Haganir, Y. Koutalos, J. Nathans, Y.-W. Peng, R. R. Reed, J. Schroeder, W.-P. Yu, and D. T.-C. Yue for discussions and comments; J. Finn for help with computer analysis and transfections; R. S. Dhallan for constructing some of the chimeras based on a method suggested by R. R. Reed; and G. Yellen for lending equipment and for first pointing out that the calcium-calmodulin-induced shift in ligand affinity of the olfactory channel may reflect a change in gating. Supported in part by NIH grant EY 06837.

15 July 1994; accepted 26 October 1994